

This discussion paper is/has been under review for the journal Atmospheric Measurement Techniques (AMT). Please refer to the corresponding final paper in AMT if available.

Comparison of GOME-2/Metop-A ozone profiles with GOMOS, OSIRIS and MLS measurements

A. Määttä¹, O. N. E. Tuinder², S. Tukiainen¹, V. Sofieva¹, and J. Tamminen¹

¹Finnish Meteorological Institute, Helsinki, Finland

²Royal Netherlands Meteorological Institute, De Bilt, the Netherlands

Received: 30 April 2015 – Accepted: 23 June 2015 – Published: 23 July 2015

Correspondence to: A. Määttä (anu.maatta@fmi.fi)

Published by Copernicus Publications on behalf of the European Geosciences Union.

AMTD

8, 7663–7695, 2015

GOME-2/Metop-A
ozone profile
comparison

A. Määttä et al.

Title Page

Abstract

Introduction

Conclusions

References

Tables

Figures

◀

▶

◀

▶

Back

Close

Full Screen / Esc

Printer-friendly Version

Interactive Discussion



Abstract

This paper presents a comparison of vertical ozone profiles retrieved by the Ozone Profile Retrieval Algorithm (OPERA) from the Global Ozone Monitoring Experiment 2 (GOME-2) measurements on board Metop-A with high-vertical-resolution ozone profiles by Global Ozone Monitoring by Occultation of Stars (GOMOS), Optical Spectrograph and Infrared Imager System (OSIRIS) and Microwave Limb Sounder (MLS). The comparison, with global coverage, focuses on the stratosphere and the lower mesosphere and covers the period from March 2008 until the end of 2011.

The comparison shows an agreement of the GOME-2 ozone profiles with those of GOMOS, OSIRIS and MLS within $\pm 15\%$ in the altitude range from 15 km up to ~ 35 –40 km depending on latitude. The GOME-2 ozone profiles from non-degradation corrected radiances have a tendency to a systematic negative bias with respect to the reference data above ~ 30 km. The GOME-2 bias with respect to the high-vertical resolution instruments depends on season, with the strongest dependence observed at high latitudes.

1 Introduction

Changes in the atmospheric ozone distribution originating from natural and anthropogenic sources have an effect on the Earth's climate. These changes are altitude dependent and thus demand the continuous monitoring of the vertical distribution of ozone in the atmosphere. Ozone depletion events in the Antarctic and occasionally also in the Arctic region, as well as long-term changes in the mid-latitude ozone, can be monitored by satellites that provide vertical ozone profiles. These satellite-based vertical ozone profiles have almost global coverage and can be applied for various applications and research areas from local phenomena to global evolution. Ozone profiles have been retrieved from various space born instruments with different sensor types and measurement techniques since 1970s (Hassler et al., 2014).

AMTD

8, 7663–7695, 2015

GOME-2/Metop-A ozone profile comparison

A. Määttä et al.

[Title Page](#)

[Abstract](#)

[Introduction](#)

[Conclusions](#)

[References](#)

[Tables](#)

[Figures](#)

◀

▶

◀

▶

[Back](#)

[Close](#)

[Full Screen / Esc](#)

[Printer-friendly Version](#)

[Interactive Discussion](#)



GOME-2/Metop-A ozone profile comparison

A. Määttä et al.

[Title Page](#)

[Abstract](#)

[Introduction](#)

[Conclusions](#)

[References](#)

[Tables](#)

[Figures](#)

[◀](#)

[▶](#)

[◀](#)

[▶](#)

[Back](#)

[Close](#)

[Full Screen / Esc](#)

[Printer-friendly Version](#)

[Interactive Discussion](#)



[Title Page](#)[Abstract](#)[Introduction](#)[Conclusions](#)[References](#)[Tables](#)[Figures](#)[◀](#)[▶](#)[◀](#)[▶](#)[Back](#)[Close](#)[Full Screen / Esc](#)[Printer-friendly Version](#)[Interactive Discussion](#)

at higher latitudes and the tropical region. The detailed validation reports (Kins and Delcloo, 2012; Delcloo and Kreher, 2013) can be found at <http://o3msaf.fmi.fi>.

In this paper the quality of the ozone profiles retrieved by OPERA using GOME-2/Metop-A measurements is assessed by comparison with profiles retrieved from Global Ozone Monitoring by Occultation of Stars (GOMOS), Optical Spectrograph and Infrared Imager System (OSIRIS) and Microwave Limb Sounder (MLS). The motivation for this comparison is to expand the evaluation of the GOME-2 ozone profiles to a good spatial coverage using high-quality satellite ozone profiles with a significantly higher vertical resolution than GOME-2. The altitude region for the comparison is between 15 and 60 km and the comparison period covers almost four full years of collocated data from March 2008 to December 2011.

The paper is organized as follows. The characteristics of the ozone profile data involved in the comparison are presented in Sects. 2 and 3. The methodology for the comparison of ozone profiles is presented in Sect. 4. Finally, the comparison results are presented and discussed in Sect. 5, and conclusions are provided in Sect. 6.

2 GOME-2 ozone profiles

Metop-A was launched on 19 October 2006 into a Sun-synchronous polar orbit at an altitude of about 840 km and is the first one in EUMETSAT's Metop series. GOME-2 aboard Metop-A is a nadir viewing scanning spectrometer using four channels in the ultraviolet (UV) and visible (VIS) range between 240 and 790 nm with a spectral resolution of 0.2–0.4 nm. The standard footprint size of the ground pixel is usually 640 km × 40 km for the UV part and 80 km × 40 km for the VIS part of the spectrum. The equator crossing local time is 09:30 a.m. for the descending node. The GOME-2 measurements are used to retrieve total column and profile of ozone, surface UV radiation, aerosols and total columns of NO₂, SO₂, BrO, HCHO and H₂O as well as tropospheric subcolumns of NO₂ and ozone (Hassinen et al., 2015; Munro et al., 2006).

The data available for retrieval of vertical ozone profiles from GOME-2 using the UV-VIS spectral range between 265 and 330 nm started in January 2007. The ozone profiles are generated by the OPERA algorithm developed at the Royal Netherlands Meteorological Institute (KNMI). The algorithm uses an iterative approach to the fitting 5 the ozone profile to the measured radiances using Optimal Estimation (Rodgers and Connor, 2003) and the LidortA radiative transfer model. The ozone climatology is used as a priori (McPeters et al., 2007). The error analysis shows that the dominant errors exceeding the 5 % level originate from uncertainties in the spectral calibration, ozone a priori and the vertical temperature profile, the cloud top pressure and forward model 10 errors (see ATBD van Oss et al., 2014, for the details).

For users there are two types products available, a Near-Real-Time Ozone Profile product consisting of 3 min data blocks within 3 h of sensing and an Offline Ozone Profile product consisting data blocks as whole orbits within 2 weeks. Both of these products are retrieved in a coarse resolution using $640\text{ km} \times 40\text{ km}$ ground pixels and 15 in a high resolution using $80\text{ km} \times 40\text{ km}$ ground pixels (see the ozone profile product user manual Tuinder, 2015). The ozone profile products are produced at KNMI and available to users in NRT via the EUMETCAST system and offline via the O3M SAF archive (<http://o3msaf.fmi.fi>). One orbit file has the observations from sun-lit side of the Earth. Global coverage can be achieved in 1.5 days with about 14 orbits daily.

In this paper, we consider the ozone profiles from the coarse resolution Level 2 offline 20 ozone profile product produced by OPERA during 2008–2011 with software versions 1.14–1.24. The ozone profile product contains the a priori profile, the averaging kernels, the full error covariance matrix, the retrieval noise covariance matrix and other relevant information (van Oss et al., 2014; Tuinder, 2015). The ozone profile is given as partial 25 columns in Dobson units (DU) at 40 layers between logarithmically spaced pressure levels between surface and 0.001 hPa (van Oss et al., 2014; Tuinder, 2015). The cloud-top pressure replaces the surface pressure level in cloudy and partially cloudy scenes.

The vertical resolution of the ozone profile retrieved using OPERA is between 8 and 11 km at its best as estimated from the averaging kernels.

GOME-2/Metop-A
ozone profile
comparison

A. Määttä et al.

Title Page

Abstract

Introduction

Conclusions

References

Tables

Figures

|◀

▶|

◀

▶

Back

Close

Full Screen / Esc

Printer-friendly Version

Interactive Discussion



3 Reference spaceborne ozone profiles used in the comparison

In this comparison study we have used reference measurements from three satellite instruments: GOMOS/Envisat, OSIRIS/Odin and MLS/Aura. These instruments have a long-term data record with ozone profiles available for a time period between 2002–
5 2012 for GOMOS, from 2001 to present for OSIRIS and from 2004 to present for MLS. Table 1 gives the short description of the data used in the comparison.

3.1 GOMOS ozone profiles

The GOMOS instrument was on board the ESA's Envisat satellite launched in 2002 and it monitored ozone, other trace gases (such as NO_2 , NO_3 , H_2O and O_2) and aerosols
10 until 2012 using stars as light sources (Bertaux et al., 2010). The spectral range in the ultraviolet-visible wavelengths of the instrument was between 248 and 690 nm. Additionally GOMOS measured at two near-infrared bands (755–774 nm and 926–954 nm).

GOMOS utilized a stellar occultation technique to measure the vertical distribution of ozone at the altitudes between 10 and 100 km (Kyrölä et al., 2010; Tamminen et al.,
15 2010). The retrieval is based on the maximum likelihood method and it does not use a priori information of the vertical distribution of ozone (Kyrölä et al., 2010).

The accuracy of the ozone profile derived from the GOMOS retrieval depends on the star magnitude and temperature of the star (Kyrölä et al., 2010; Tamminen et al.,
20 2010). The most accurate ozone profiles are retrieved using the hot and bright stars (Kyrölä et al., 2010). The GOMOS nighttime measurements have a good precision with a retrieval error in the stratosphere around 0.5–4 % and in the mesosphere around 2–10 % (Tamminen et al., 2010). The stratospheric ozone precision estimates from the GOMOS nighttime measurements has been validated by using the differential method presented by Sofieva et al. (2014). The summary of the geophysical validation of GOMOS measurements is presented in Bertaux et al. (2010).

In this comparison study, we have used nighttime ozone profiles from the GOMOS processor version 6 data (see Table 1). We have selected only stars that are medium

AMTD

8, 7663–7695, 2015

GOME-2/Metop-A ozone profile comparison

A. Määttä et al.

[Title Page](#)

[Abstract](#)

[Introduction](#)

[Conclusions](#)

[References](#)

[Tables](#)

[Figures](#)

◀

▶

◀

▶

[Back](#)

[Close](#)

[Full Screen / Esc](#)

[Printer-friendly Version](#)

[Interactive Discussion](#)



to bright (magnitude $M_V \leq 2$) and stars that are hot (temperature ≥ 7000 K). The collocation criteria for the comparison are a distance ≤ 400 km between the GOME-2 pixel center and GOMOS measurement ground location, and ± 12 h for the maximum time difference.

5 3.2 OSIRIS ozone profiles

OSIRIS on board the Swedish Odin satellite was launched in 2001 (Llewellyn et al., 2004). OSIRIS measures limb scattered solar light at 280–810 nm region with a spectral resolution of ~ 1 nm. OSIRIS has also infrared imager. From the OSIRIS measurements various trace gases can be retrieved, such as ozone, NO₂, OCIO, BrO and aerosols. The OSIRIS measures near 06:00 p.m. local solar time on the ascending node and near 06:00 a.m. local solar time on the descending node.

10 The ozone profile dataset used in this comparison comes from the FMI-OSIRIS Level 2 product (version 3) using the latest OSIRIS Level 1 data. The ozone profiles in the FMI-OSIRIS product are retrieved using a Onion Peeling type inversion method (Tukiainen et al., 2008) developed at the Finnish Meteorological Institute (FMI). The basic 15 difference between this inversion method and the other retrieval methods using OSIRIS data, e.g. OSIRIS SaskMART, is that it uses the whole ultraviolet-visible spectrum to produce ozone vertical profiles between 15 and 70 km (Tukiainen et al., 2008). The one year intercomparison between GOMOS nighttime and FMI-OSIRIS daytime ozone profiles 20 in the altitude range of 21–45 km and at latitudes 35° S–35° N showed a maximum of 5 % median relative difference (Tukiainen et al., 2008).

25 For the comparison, we have used OSIRIS data separated by a maximum distance of 200 km between the center of the GOME-2 pixel maximum ± 6 h in time. In addition, we restricted the dataset to the morning (sunrise) measurements in order to have the collocations near the local solar time of the GOME-2 measurements.

AMTD

8, 7663–7695, 2015

GOME-2/Metop-A ozone profile comparison

A. Määttä et al.

[Title Page](#)

[Abstract](#)

[Introduction](#)

[Conclusions](#)

[References](#)

[Tables](#)

[Figures](#)

◀

▶

◀

▶

[Back](#)

[Close](#)

[Full Screen / Esc](#)

[Printer-friendly Version](#)

[Interactive Discussion](#)



3.3 MLS ozone profiles

The MLS instrument flies on board the Earth Observing System (EOS) Aura satellite and was launched in 2004 (Waters et al., 2006). MLS measures microwave thermal emission from limb. Retrieved from the MLS measurements are vertical profiles of trace gases including ozone, BrO, ClO, CO, H₂O, HCl, HCN, HNO₃, N₂O and SO₂. Ozone is retrieved using the 240 GHz spectral region. The vertical ozone profiles are reported as mixing ratios at pressure levels. The useful pressure range for the MLS ozone profiles is between 215 and 0.02 hPa. The comparison in this paper includes MLS version 3.3 Level 2 ozone profiles (Livesey et al., 2011). The MLS ozone comparison in the stratosphere with other profiles from satellite, balloon, aircraft and ground-based data gave the overall 5–10 % agreement (Livesey et al., 2011).

The collocation criteria used allow the maximum distance between GOME-2 pixel center and MLS to be 100 km and a maximum time difference of ±6 h between the sensing times.

15 4 Comparison methodology

First, we converted GOMOS, OSIRIS and MLS vertical ozone profiles into the representation of GOME-2, i.e., into partial columns at GOME-2 pressure layers.

Then we have smoothed the high-resolution profiles by GOMOS, OSIRIS and MLS to the GOME-2 vertical resolution using the GOME-2 averaging kernels according to Rodgers and Connor (2003):

$$x_{\text{sref}} = \mathbf{A} x_{\text{ref}} + (\mathbf{I} - \mathbf{A}) x_a = x_a + \mathbf{A}(x_{\text{ref}} - x_a), \quad (1)$$

where x_{sref} is the resulting smoothed reference profile, x_{ref} is the actual reference profile interpolated to the GOME-2 pressure layers, x_a is a priori profile and \mathbf{A} is the averaging kernel matrix in the GOME-2 retrieval. In this form the smoothed reference

AMTD

8, 7663–7695, 2015

GOME-2/Metop-A ozone profile comparison

A. Määttä et al.

[Title Page](#)

[Abstract](#)

[Introduction](#)

[Conclusions](#)

[References](#)

[Tables](#)

[Figures](#)

[◀](#)

[▶](#)

[◀](#)

[▶](#)

[Back](#)

[Close](#)

[Full Screen / Esc](#)

[Printer-friendly Version](#)

[Interactive Discussion](#)



profile is expressed as a linear combination of the reference profile (as a “true profile”) and a priori profile with matrix weights \mathbf{A} and $(\mathbf{I} - \mathbf{A})$, respectively.

We have performed the comparison between temporally and spatially coincident profiles only. The collocation criteria for each reference instrument are described in Sects. 3.1–3.3. While the calculation is done at the GOME-2 pressure layers, the results are shown in the altitude range of 15–60 km. As the altitude layers in km vary slightly among the retrieved GOME-2 profiles, we have presented in figures the ozone layer amounts at the midpoints of the averaged altitude layers.

The relative difference (%) used here is defined as

$$10 \quad RD = \frac{\text{GOME-2} - \text{REF}}{\text{REF}} \times 100\% \quad (2)$$

where the ozone profiles GOME-2 and REF are in the unit of partial ozone columns in DU at 40 pressure layers.

5 Comparison results and discussion

5.1 Latitude dependent difference

15 A general view of the agreement of vertical ozone profiles retrieved from GOME-2 measurements, which are not corrected for instrument degradation, with respect to the reference profiles covering the whole time period is shown in Fig. 1.

20 The vertical pattern of the mean relative differences across the tropical and mid-latitude regions are similar in comparison with all three instruments. On average, the GOME-2 ozone profiles are overestimated from the surface up to ~ 25 km and underestimated above around 30 km apart from the higher latitudes. The agreement between the GOME-2 and reference ozone profiles is the best at midlatitudes. Around the equator, between 20° S and 20° N, there is a higher positive bias reaching 20 % at lower altitudes below ~ 20 km.

Title Page	
Abstract	Introduction
Conclusions	References
Tables	Figures
◀	▶
◀	▶
Back	Close
Full Screen / Esc	
Printer-friendly Version	
Interactive Discussion	



At southern high latitudes the averaged relative differences between GOME-2 and the reference profiles are significantly different from the mid-latitudes and tropics, and they are also different from each other. This difference can be explained by a sampling issue related to a seasonal dependence at high latitudes as verified below in Sect. 5.2.

- 5 The overestimation with respect to the GOMOS data at the southern high latitudes at altitude range \sim 30–40 km occurs during August and September, and these months are dominating the average difference. This positive difference can also be seen in the Fig. 2 regarding season JJA (i.e. June, July and August) when there is actually collocated data from August only. With respect to the OSIRIS data in the zone 65–
10 75° S there was also detected overestimation during August but is not seen in the averaged values since GOME-2 underestimates ozone at other times. At the same time, the comparison with MLS data (top right panel in Fig. 1) shows an overestimation at altitude range \sim 25–40 km between 75 and 85° S and at altitude range \sim 18–28 km
15 between 65 and 75° S that is not encountered when compared against GOMOS and OSIRIS data. On the other hand, in the zone 55–65° S there is a positive bias up to about 28 km with respect to MLS data in summer and the positive bias is also found with respect to OSIRIS data in the summer season. When averaged over years, this bias disappears.

5.2 Seasonal dependence and temporal evolution of the difference

- 20 The seasonal variation of the profiles of mean relative difference of GOME-2 ozone profiles vs. GOMOS, OSIRIS and MLS profiles are shown in Figs. 2–4. In these plots, the collocated data is divided into five latitude zones. The seasons are defined as DJF (December, January, February), MAM (March, April, May), JJA (June, July, August) and SON (September, October, November). Here we consider only two years of data: 2010 and 2011.
25

At tropical latitudes (30° S– 30° N) the negative peak of relative difference just above 40 km is on average about 10 % deeper in DJF than in the other seasons. The seasonal variation of the mean relative difference is low at the tropical latitudes, which

Title Page	
Abstract	Introduction
Conclusions	References
Tables	Figures
◀	▶
◀	▶
Back	Close
Full Screen / Esc	
Printer-friendly Version	
Interactive Discussion	



**GOME-2/Metop-A
ozone profile
comparison**

A. Määttä et al.

[Title Page](#)[Abstract](#)[Introduction](#)[Conclusions](#)[References](#)[Tables](#)[Figures](#)[|◀](#)[▶|](#)[◀](#)[▶](#)[Back](#)[Close](#)[Full Screen / Esc](#)[Printer-friendly Version](#)[Interactive Discussion](#)

after April 2010. These changes correspond to OPERA algorithm and software version updates (Tuinder, 2015).

There can be several possible reasons for the mainly systematic differences encountered with respect to the reference data. Low ozone concentrations at higher altitude layers produce more easily rather high bias percentage values.

The GOME-2 ozone profiles and the reference profiles used from the GOMOS, OSIRIS and MLS instruments are collocated at different local solar times (see Table 1). It has been shown that the natural variability of ozone is affected by the photo-chemical reactions using solar light above 40 km (e.g. Studer et al., 2014; Sakazaki et al., 2013). The large relative differences in the upper stratosphere with respect to GOMOS data, and to a lesser extent against OSIRIS and MLS data, could be caused, at least partly, by this diurnal effect (see Fig. 8).

The comparisons done here with occultation and limb measurements show a turning point with the maximum relative differences at around 40–50 km. In the paper by van Peet et al. (2014) it is discussed that at a region above an altitude of 2 hPa (~ 45 km) the implemented additive offset (to partially correct the influence of instrument degradation) has the largest influence in the number of retrieved pixels passing quality criterion, whereas the validation results shown in this paper it does not have significant effect. In the validation report (Delcloo and Kreher, 2013) it has been noticed that in the course of time the GOME-2/MetopA data has become noisier due to the instrument degradation.

5.3 Solar zenith angle dependent difference

We have studied the dependence of GOME-2 biases on solar zenith angle (SZA) provided with each GOME-2 ozone profile retrieval. Figures 9 and 10 show SZA dependence of the relative differences between GOMOS and OSIRIS data for the altitude layers located around 23, 30, 37 and 45 km at the southern high latitudes.

At the southern high latitudes the negative bias increases with increasing SZA around 23 km altitude. This is also observed at northern high latitudes, 60–90° N (not shown here). The similar dependence on SZA at tropical and mid-latitude regions was

[Title Page](#)[Abstract](#)[Introduction](#)[Conclusions](#)[References](#)[Tables](#)[Figures](#)[|◀](#)[▶|](#)[◀](#)[▶](#)[Back](#)[Close](#)[Full Screen / Esc](#)[Printer-friendly Version](#)[Interactive Discussion](#)

registered around 45 km. On the contrary, at the southern mid-latitudes around 37 km there is tendency for the (negative) bias to get smaller, i.e. getting a better agreement, when the SZA increases.

- In Figs 9 and 10 exceptionally large positive relative differences with respect to both GOMOS and OSIRIS data appear above ~ 30 km when $SZA > 85^\circ$ and at the same time large negative differences occur around 23 km. In addition, the very high positive relative differences with respect to OSIRIS profiles (Fig. 10) are encountered when SZA is between 68 and 80° . This happens only in the southernmost latitude levels around 87° S during the southern polar spring and summer months. The collocated pixels with GOMOS data have the southernmost latitudes around 69° S thus these high difference values are not seen against GOMOS data (Fig. 9).

5.4 Arctic ozone depletion 2011

- In order to demonstrate the usefulness of the GOME-2 data we considered the ozone profiles retrieved from the GOME-2 measurements during the Arctic ozone depletion in spring 2011. In the Antarctic region the ozone hole event recurs annually, but in the Arctic region severe ozone loss happens less frequently. The exceptionally reduced transport of ozone from mid-latitudes into the Arctic region together with enhanced chemical ozone loss inside polar vortex caused the anomalously low ozone concentration over the North Pole in March 2011 (Manney et al., 2011; Isaksen et al., 2012). The Arctic ozone depletion is not represented by the typical a priori profile used for this season and latitude and hereby offers a chance to verify the retrieved profiles under the challenging circumstances.

As the air masses inside the polar vortex can be very different compared to outside polar vortex atmosphere, the comparisons have been done separately for the pixels being inside and outside polar vortex. We have done the comparison over Arctic region (60 – 90° N) with collocated OSIRIS data and used 475 K potential vorticity to determine the collocated GOME-2 pixel to be outside or inside polar vortex area. In this special case, we require pixels to a $SZA \leq 65^\circ$ because the disagreement with reference

[Title Page](#)[Abstract](#)[Introduction](#)[Conclusions](#)[References](#)[Tables](#)[Figures](#)[|◀](#)[▶|](#)[◀](#)[▶](#)[Back](#)[Close](#)[Full Screen / Esc](#)[Printer-friendly Version](#)[Interactive Discussion](#)

[Title Page](#)[Abstract](#)[Introduction](#)[Conclusions](#)[References](#)[Tables](#)[Figures](#)[|◀](#)[▶|](#)[◀](#)[▶](#)[Back](#)[Close](#)[Full Screen / Esc](#)[Printer-friendly Version](#)[Interactive Discussion](#)

data increases as SZA increases at high latitudes when considering the altitude range around 20 km (see previous Sect. 5.3).

Figure 11 shows the monthly averages for March 2011 of collocated ozone profiles from GOME-2 and OSIRIS measurements separately for profiles inside (left hand panel) and outside polar vortex (middle panel). The number of collocated profiles inside vortex is 17 and outside vortex 96, respectively. In reality, as the division is not the same at all altitudes, some part of the profile can be inside and rest of the profile outside polar vortex.

The difference between inside and outside polar vortex monthly means scaled by outside polar vortex monthly mean is evident as seen for GOME-2 (blue) and OSIRIS (black) (Fig. 11 right panel).

This case study shows that the GOME-2 can observe the ozone depletion well and thus provides the very useful information. We have to note, that the horizontal coverage by GOME-2 is much more dense than by limb-viewing instruments.

5.5 Correction for instrumental degradation

The GOME-2 vertical ozone profile algorithm depends strongly on good absolute-calibrated solar and earthshine spectra. Unfortunately, GOME-2 is affected by instrument degradation which is strongest in the UV. This instrumental degradation increases over time, thus setting additional challenges to the algorithm to adapt to these changes.

An experimental correction has been developed, which aims to rectify an initial bias and the time dependent degradation for a number of relevant wavelengths and scan angles.

To demonstrate its potential we have done some comparison of GOME-2 vertical ozone profiles using newly developed experimental degradation correction with the GOMOS, OSIRIS and MLS data. The preliminary results for March 2008, shown in Fig. 12, indicate good functionality of the implemented correction. The large underestimation of ozone above 40 km has been turned into a smaller overestimation, rectifying the deviation considerably. The operational ozone profiles (dashed curves) used here are from the original offline ozone product (OOP) in coarse resolution horizontal resolu-

tion whereas the new degradation corrected profiles (solid curves) have been retrieved in higher resolution. Thus the number of collocated profiles in comparison is higher when using higher resolution GOME-2 data. Since the beginning of the O3M SAF, the operationally available vertical ozone profile product has been under the continuous development and improvement (Tuinder, 2015). This can be seen also in time line comparison results of the upper stratosphere, e.g. after 2010 (Figs. 5–7).

6 Conclusions

We have evaluated the performance of the GOME-2 ozone profiles that are based on measurements that are not corrected for instrument degradation. This was done on a global scale by comparing GOME-2 ozone profiles with high-vertical resolution ozone profiles by GOMOS, OSIRIS and MLS. In this comparison study, we have used spatially and temporally coincident profiles for the time period of March 2008 until December 2011. In the analysis, we presented the reference high-vertical-resolution profiles in the resolution of GOME-2.

The overall agreement of ozone profiles from GOME-2 and other instruments is within 15 % below 35–40 km. The vertical pattern of the biases with respect to reference data depends on latitude and season. The comparison shows that GOME-2 profiles have a tendency to underestimate the ozone concentration above ~ 30 km. On the other hand, GOME-2 systematically overestimates in the lower stratosphere at tropical and mid-latitudes. At high latitudes, the bias as a function of altitude shows a wider variation among the different seasons.

The special case considering the exceptional ozone depletion at Arctic during the spring 2011 showed that the GOME-2 ozone profiles captured the unusual ozone vertical structure in spite of an a priori ozone profile that was not representative of that situation. This indicates that GOME-2 data can provide valuable geophysical information.

GOME-2/Metop-A ozone profile comparison

A. Määttä et al.

[Title Page](#)

[Abstract](#)

[Introduction](#)

[Conclusions](#)

[References](#)

[Tables](#)

[Figures](#)

◀

▶

◀

▶

[Back](#)

[Close](#)

[Full Screen / Esc](#)

[Printer-friendly Version](#)

[Interactive Discussion](#)



GOME-2/Metop-A ozone profile comparison

A. Määttä et al.

[Title Page](#)

[Abstract](#)

[Introduction](#)

[Conclusions](#)

[References](#)

[Tables](#)

[Figures](#)

◀

▶

◀

▶

[Back](#)

[Close](#)

[Full Screen / Esc](#)

[Printer-friendly Version](#)

[Interactive Discussion](#)



Acknowledgements. The GOME-2 vertical ozone profiles are provided by EUMETSAT's Satellite Application Facility for Atmospheric Composition and UV Radiation (O3M SAF). The authors would like to thank the GOMOS, FMI-OSIRIS and MLS data providers for data availability. This work has been done in the context of the O3M SAF project and the Academy of Finland INQUIRE and ASTREX projects.

References

- Bertaux, J. L., Kyrölä, E., Fussen, D., Hauchecorne, A., Dalaudier, F., Sofieva, V., Tamminen, J., Vanhellemont, F., Fanton d'Andon, O., Barrot, G., Mangin, A., Blanot, L., Lebrun, J. C., Pérot, K., Fehr, T., Saavedra, L., Leppelmeier, G. W., and Fraisse, R.: Global ozone monitoring by occultation of stars: an overview of GOMOS measurements on ENVISAT, *Atmos. Chem. Phys.*, 10, 12091–12148, doi:10.5194/acp-10-12091-2010, 2010. 7668
- Callies, J., Corpaccioli, E., Eisinger, M., Hahne, A., and Lefebvre, A.: GOME-2 – Metop's second-generation sensor for operational ozone monitoring, *ESA Bull.-Eur. Space.*, 102, 28–36, 2000. 7665
- Delcloo, A. and Kreher, K.: O3M SAF Validation Report for Near-Real-Time Ozone Profile, Offline Ozone Profile, Near-Real-Time High Resolution Ozone Profile and Offline High Resolution Ozone Profile products, SAF/O3M/RMI&DWD/VR/001, Ozone SAF Validation reports, O3M SAF, available at: http://o3msaf.fmi.fi/docs/vr/Validation_Report_NOP_NHP_OOP_OHP_Jun_2013.pdf (last access: 20 July 2015), 2013. 7666, 7674
- Hassinen, S., Balis, D., Bauer, H., Begoin, M., Delcloo, A., Eleftheratos, K., Gimeno Garcia, S., Granville, J., Grossi, M., Hao, N., Hedelt, P., Hendrick, F., Hess, M., Heue, K.-P., Hovila, J., Jønch-Sørensen, H., Kalakoski, N., Kiemle, S., Kins, L., Koukouli, M. E., Kujanpää, J., Lambert, J.-C., Lerot, C., Loyola, D., Määttä, A., Pedergnana, M., Pinardi, G., Romahn, F., van Roozendael, M., Lutz, R., De Smedt, I., Stammes, P., Steinbrecht, W., Tamminen, J., Theys, N., Tilstra, L. G., Tuinder, O. N. E., Valks, P., Zerefos, C., Zimmer, W., and Zyrichidou, I.: Overview of the O3M SAF GOME-2 operational atmospheric composition and UV radiation data products and data availability, *Atmos. Meas. Tech. Discuss.*, 8, 6993–7056, doi:10.5194/amt-8-6993-2015, 2015. 7666
- Hassler, B., Petropavlovskikh, I., Staehelin, J., August, T., Bhartia, P. K., Clerbaux, C., Degeenstein, D., Mazière, M. De, Dinelli, B. M., Dudhia, A., Dufour, G., Frith, S. M., Froide-

GOME-2/Metop-A ozone profile comparison

A. Määttä et al.

[Title Page](#)

[Abstract](#)

[Introduction](#)

[Conclusions](#)

[References](#)

[Tables](#)

[Figures](#)

[|◀](#)

[▶|](#)

[◀](#)

[▶](#)

[Back](#)

[Close](#)

[Full Screen / Esc](#)

[Printer-friendly Version](#)

[Interactive Discussion](#)



vaux, L., Godin-Beekmann, S., Granville, J., Harris, N. R. P., Hoppel, K., Hubert, D., Kaisai, Y., Kurylo, M. J., Kyrölä, E., Lambert, J.-C., Levelt, P. F., McElroy, C. T., McPeters, R. D., Munro, R., Nakajima, H., Parrish, A., Raspollini, P., Remsberg, E. E., Rosenlof, K. H., Rozanov, A., Sano, T., Sasano, Y., Shiotani, M., Smit, H. G. J., Stiller, G., Tamminen, J., Tarasick, D. W., Urban, J., van der A, R. J., Veefkind, J. P., Vigouroux, C., von Clarmann, T., von Savigny, C., Walker, K. A., Weber, M., Wild, J., and Zawodny, J. M.: Past changes in the vertical distribution of ozone – Part 1: Measurement techniques, uncertainties and availability, *Atmos. Meas. Tech.*, 7, 1395–1427, doi:10.5194/amt-7-1395-2014, 2014. 7664

Isaksen, I. S. A., Zerefos, C., Wang, W.-C., Balis, D., Eleftheratos, K., Rognerud, B., Stordal, F., Berntsen, T. K., LaCasce, J. H., Søvde, O. A., Olivé, D., Orsolini, Y. J., Zyrichidou, I., Prather, M., and Tuinder, O. N. E.: Attribution of the Arctic ozone column deficit in March 2011, *Geophys. Res. Lett.*, 39, L24810, doi:10.1029/2012GL053876, 2012. 7675

Kins, L. and Delcloo, A.: O3M SAF Validation Report for Near-Real-Time Ozone Profile, Offline Ozone Profile, Near-Real-Time High Resolution Ozone Profile and Offline High Resolution Ozone Profile products, SAF/O3M/DWD/VR/OOP/091, Ozone SAF Validation reports, O3M SAF, available at: http://o3msaf.fmi.fi/docs/vr/Validation_Report_NOP_NHP_OOP_OHP_Feb_2012.pdf (last access: 20 July 2015), 2012. 7666

Kyrölä, E., Tamminen, J., Sofieva, V., Bertaix, J. L., Hauchecorne, A., Dalaudier, F., Fussen, D., Vanhellemont, F., Fanton d'Andon, O., Barrot, G., Guirlet, M., Mangin, A., Blanot, L., Fehr, T., Saavedra de Miguel, L., and Fraisse, R.: Retrieval of atmospheric parameters from GOMOS data, *Atmos. Chem. Phys.*, 10, 11881–11903, doi:10.5194/acp-10-11881-2010, 2010. 7668, 7683

Livesey, N. J., Read, W. G., Froidevaux, L., Lambert, A., Manney, G. L., Pumphrey, H. C., Santere, M. L., Schwartz, M. J., Wang, S., Cofeld, R. E., Cuddy, D. T., Fuller, R. A., Jarnot, R. F., Jiang, J. H., Knosp, B. W., Stek, P. C., Wagner, P. A., and Wu, D. L.: EOS MLS Version 3.3 Level 2 data quality and description document, JPL D-33509, Jet Propulsion Laboratory, Version 3.3x-1.0, available at: http://mls.jpl.nasa.gov/data/v3-3_data_quality_document.pdf (last access: 20 July 2015), 2011. 7670, 7683

Llewellyn, E. J., Lloyd, N. D., Degenstein, D. A., Gattigner, R. L., Petelina, S. V., Bourassa, A. E., Wiensz, J. T., Ivanov, E. V., McDade, I. C., Solheim, B. H., McConnell, J. C., Haley, C. S., von Savigny, C., Sioris, C. E., McLinden, C. A., Griffioen, E., Kaminski, J., Evans, W. F. J., Puckrin, E., Strong, K., Wehrle, V., Hum, R. H., Kendall, D. J. W., Matsushita, J., Murtagh, D. P., Brohede, S., Stegman, J., Witt, G., Barnes, G., Payne, W. F., Piché, L., Smith, K., War-

shaw, G., Deslauniers, D.-L., Marchand, P., Richardson, E. H., King, R. A., Wevers, I., McCreathe, W., Kyrölä, E., Oikarinen, L., Leppelmeier, G. W., Auvinen, H., Mégie, G., Hauchecorne, A., Lefèvre, F., de La Nöe, J., Ricaud, P., Frisk, U., Sjoberg, F., Von Schéele, F., and Nordh, L.: The OSIRIS instrument on the Odin spacecraft, *Can. J. Phys.*, 82, 411–422, doi:10.1139/P04-005, 2004. 7669

5 Manney, G. L., Santee, M. L., Rex, M., Livesey, N. J., Pitts, M. C., Veefkind, P., Nash, E. R., Wohltmann, I., Lehmann, R., Froidevaux, L., Poole, L. R., Schoeberl, M. R., Haffner, D. P., Davies, J., Dorokhov, V., Gernhardt, H., Johnson, B., Kivi, R., Kyrö, E., Larsen, N., Levelt, P. F., Makshtas, A., McElroy, C. T., Nakajima, H., Parrondo, M. C., Tarasick, D. W., von der Gathen, P., Walker, K. A., and Zinoviev, N. S.: Unprecedented Arctic ozone loss in 2011, *Nature*, 478, 469–475, doi:10.1038/nature10556, 2011. 7675

10 McPeters, R. D., Labow, G. J., and Logan, J. A.: Ozone climatological profiles for satellite retrieval algorithms, *J. Geophys. Res.*, 112, D05308, doi:10.1029/2005JD006823, 2007. 7667

15 Mijling, B., Tuinder, O. N. E., van Oss, R. F., and van der A, R. J.: Improving ozone profile retrieval from spaceborne UV backscatter spectrometers using convergence behaviour diagnostics, *Atmos. Meas. Tech.*, 3, 1555–1568, doi:10.5194/amt-3-1555-2010, 2010. 7665

20 Munro, R., Eisinger, M., Anderson, C., Callies, J., Corpaccioli, E., Lang, R., Lefebvre, A., Livschitz, Y., and Albinana, A. P.: GOME-2 on MetOp: From in-orbit verification to routine operations, in: Proceedings of EUMETSAT Meteorological Satellite Conference, Helsinki, Finland, 12–16 June 2006, p. 48, 2006. 7666

25 Munro, R., Lang, R., Klaes, D., Poli, G., Retscher, C., Lindstrot, R., Huckle, R., Lacan, A., Grzegorski, M., Holdak, A., Kokhanovsky, A., Livschitz, J., and Eisinger, M.: The GOME-2 instrument on the Metop series of satellites: instrument design, calibration, and level 1 data processing – an overview, *Atmos. Meas. Tech. Discuss.*, in press, 2015. 7665

30 Rodgers, C. D. and Connor, B. J.: Intercomparison of remote sounding instruments, *J. Geophys. Res.*, 108, 4116, doi:10.1029/2002JD002299, 2003. 7667, 7670

Sakazaki, T., Fujiwara, M., Mitsuda, C., Imai, K., Manago, N., Naito, Y., Nakamura, T., Akiyoshi, H., Kinnison, D., Sano, T., Suzuki, M., and Shiotani, M.: Diurnal ozone variations in the stratosphere revealed in observations from the Superconducting Submillimeter-Wave Limb-Emission Sounder (SMILES) on board the International Space Station (ISS), *J. Geophys. Res.*, 118, 2991–3006, doi:10.1002/jgrd.50220, 2013. 7674

Sofieva, V. F., Tamminen, J., Kyrölä, E., Laeng, A., von Clarmann, T., Dalaudier, F., Hauchecorne, A., Bertaux, J.-L., Barrot, G., Blanot, L., Fussen, D., and Vanhellemont, F.: 7680

GOME-2/Metop-A ozone profile comparison

A. Määttä et al.

[Title Page](#)

[Abstract](#)

[Introduction](#)

[Conclusions](#)

[References](#)

[Tables](#)

[Figures](#)

◀

▶

◀

▶

[Back](#)

[Close](#)

[Full Screen / Esc](#)

[Printer-friendly Version](#)

[Interactive Discussion](#)



GOME-2/Metop-A ozone profile comparison

A. Määttä et al.

Title Page

Abstract

Introduction

Conclusions

References

Tables

Figures

◀

▶

◀

▶

Back

Close

Full Screen / Esc

Printer-friendly Version

Interactive Discussion



Validation of GOMOS ozone precision estimates in the stratosphere, *Atmos. Meas. Tech.*, 7, 2147–2158, doi:10.5194/amt-7-2147-2014, 2014. 7668

Studer, S., Hocke, K., Schanz, A., Schmidt, H., and Kämpfer, N.: A climatology of the diurnal variations in stratospheric and mesospheric ozone over Bern, Switzerland, *Atmos. Chem. Phys.*, 14, 5905–5919, doi:10.5194/acp-14-5905-2014, 2014. 7674

Tamminen, J., Kyrölä, E., Sofieva, V. F., Laine, M., BERTAUX, J.-L., Hauchecorne, A., Dalaudier, F., Fussen, D., Vanhellemont, F., Fanton-d'Andon, O., Barrot, G., Mangin, A., Guillet, M., Blanot, L., Fehr, T., Saavedra de Miguel, L., and Fraisse, R.: GOMOS data characterisation and error estimation, *Atmos. Chem. Phys.*, 10, 9505–9519, doi:10.5194/acp-10-9505-2010, 2010. 7668

Tuinder, O.: O3M SAF Product User Manual, Near Real Time and Offline Ozone Profile Products, O3MSAF/KNMI/PUM/001, O3MSAF Product User Manual, O3M SAF available at: http://o3msaf.fmi.fi/docs/pum/Product_User_Manual_NOP_OOP_May_2015.pdf (last access: 20 July 2015), 2015. 7667, 7674, 7677

Tukiainen, S., Hassinen, S., Seppälä, A., Auvinen, H., Kyrölä, E., Tamminen, J., Haley, C. S., Lloyd, N., and Verronen, P. T.: Description and validation of a limb scatter retrieval method for Odin/OSIRIS, *J. Geophys. Res.*, 113, D04308, doi:10.1029/2007JD008591, 2008. 7669, 7683

van Oss, R., de Haan, J., Tuinder, O., and Delcloo, A.: O3M SAF Algorithm Theoretical Basis Document, ATBD for the NRT and Offline Ozone Profile Products, O3MSAF/KNMI/ATBD/001, O3MSAF Algorithm Theoretical Basis Document, O3M SAF available at: http://o3msaf.fmi.fi/docs/atbd/Algorithm_Theoretical_Basis_Document_NOP_OOP_Nov_2014.pdf (last access: 20 July 2015), 2014. 7667, 7683

van Peet, J. C. A., van der A, R. J., Tuinder, O. N. E., Wolfram, E., Salvador, J., Levelt, P. F., and Kelder, H. M.: Ozone ProfilE Retrieval Algorithm (OPERA) for nadir-looking satellite instruments in the UV–VIS, *Atmos. Meas. Tech.*, 7, 859–876, doi:10.5194/amt-7-859-2014, 2014. 7665, 7674

Waters, J. W., Froidevaux, L., Harwood, R. S., Jarnot, R. F., Pickett, H. M., Read, W. G., Siegel, P. H., Cofield, R. E., Filipiak, M. J., Flower, D. A., Holden, J. R., Lau, G. K., Livesey, N. J., Manney, G. L., Pumphrey, H. C., Santee, M. L., Wu, D. L., Cuddy, D. T., Lay, R. R., Loo, M. S., Perun, V. S., Schwartz, M. J., Stek, P. C., Thurstans, R. P., Boyles, M. A., Chandra, K. M., Chavez, M. C., Chen, G.-S., Chudasama, B. V., Dodge, R., Fuller, R. A., Girard, M. A., Jiang, J. H., Jiang, Y., Knosp, B. W., LaBelle, R. C., Lam, J. C.,

GOME-2/Metop-A
ozone profile
comparison

A. Määttä et al.

Title Page	
Abstract	Introduction
Conclusions	References
Tables	Figures
◀	▶
◀	▶
Back	Close
Full Screen / Esc	
Printer-friendly Version	
Interactive Discussion	



GOME-2/Metop-A ozone profile comparison

A. Määttä et al.

Table 1. Description of ozone profile data used in this paper.

Instrument	GOME-2	GOMOS	OSIRIS	MLS
Principle	nadir scatter	star occultation	limb scatter	limb thermal emission
Local time	~09:30 a.m.	~10:00 p.m. outside polar area	~06:00 a.m. and 06:00 p.m.	~01:45 p.m.
Algorithm	OPERA ¹	IPF6.0 ²	MOP ³	MLS v3.3 ⁴
Ozone unit	layer partial column in DU	number density	number density	volume mixing ratio
Vertical levels	41	100–150	25–60	37–47
Vertical resolution	8–11 km, depending on altitude	2–3 km, depending on altitude	2–3 km, depending on altitude	2.5–3 km

¹ van Oss et al. (2014), ² Kyrölä et al. (2010), ³ Tukiainen et al. (2008), ⁴ Livesey et al. (2011).

Title Page

Abstract

Introduction

Conclusions

References

Tables

Figures



◀

▶

Back

Close

Full Screen / Esc

Printer-friendly Version

Interactive Discussion



GOME-2/Metop-A ozone profile comparison

A. Määttä et al.

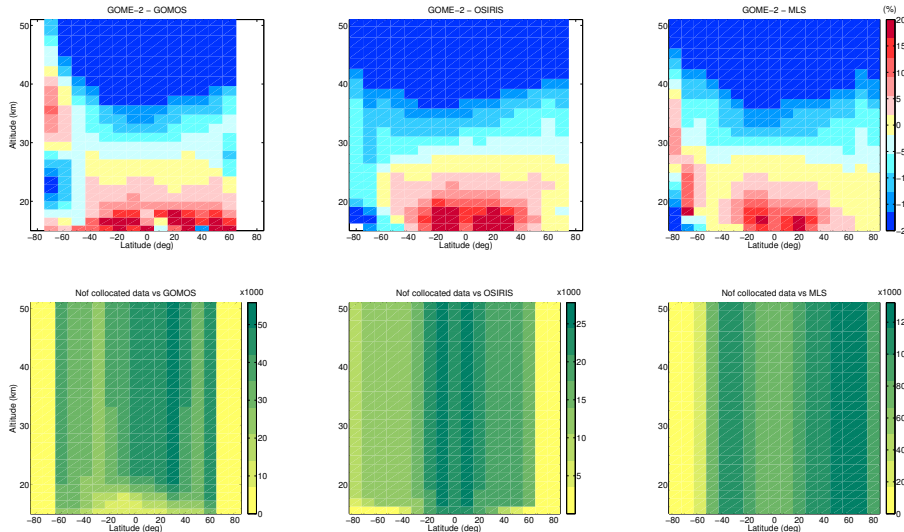


Figure 1. Top: the mean relative differences (%) at 10° latitude bins of GOME-2 and the smoothed GOMOS, OSIRIS and MLS profiles, for the full comparison period from March 2008 until December 2011. The mean profile is missing if there are less than ten collocated profile pairs. Bottom: the number of collocated profiles with GOMOS, OSIRIS and MLS, at each altitude layer.

[Title Page](#)

[Abstract](#)

[Introduction](#)

[Conclusions](#)

[References](#)

[Tables](#)

[Figures](#)

◀

▶

[Back](#)

[Close](#)

[Full Screen / Esc](#)

[Printer-friendly Version](#)

[Interactive Discussion](#)

GOME-2/Metop-A ozone profile comparison

A. Määttä et al.

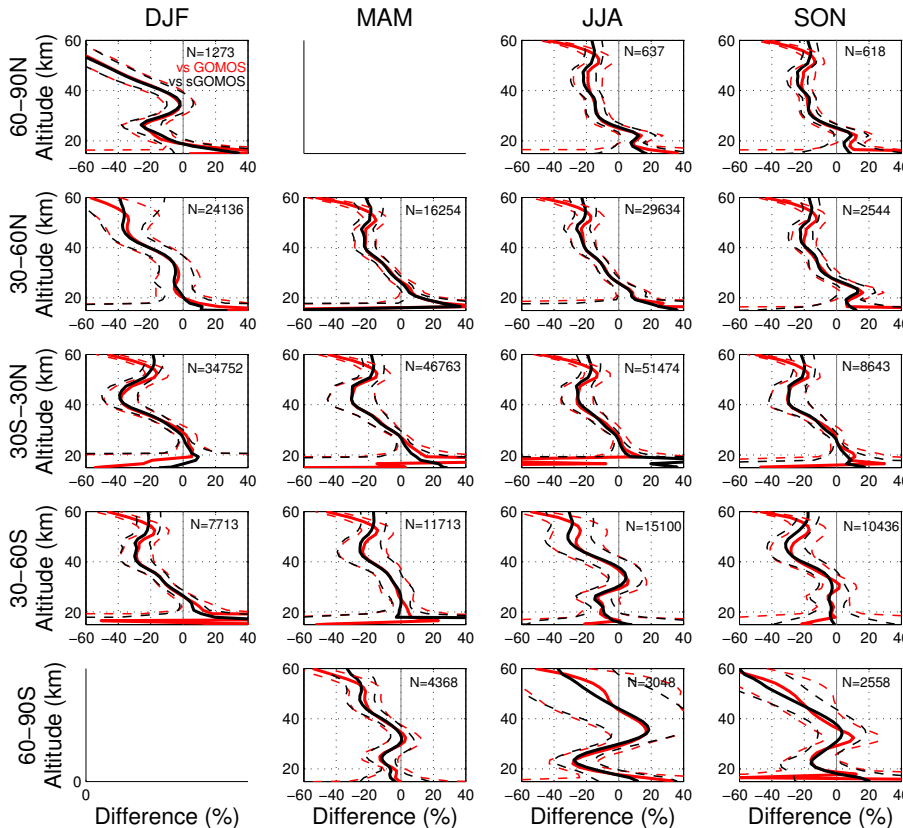


Figure 2. The mean relative differences (%) between GOME-2 and GOMOS ozone profiles classified according to the latitude zones (rows) and the seasons (columns) covering years 2010–2011 of collocated data. The comparison results are shown against the smoothed GO-MOS profiles (black) and the actual GOMOS profiles (red). The dashed lines show the 1σ standard deviation around the mean. The number of collocated profile pairs is given in the upper right corner of each panel.

[Title Page](#)

[Abstract](#)

[Introduction](#)

[Conclusions](#)

[References](#)

[Tables](#)

[Figures](#)

◀

▶

◀

▶

[Back](#)

[Close](#)

[Full Screen / Esc](#)

[Printer-friendly Version](#)

[Interactive Discussion](#)

GOME-2/Metop-A ozone profile comparison

A. Määttä et al.

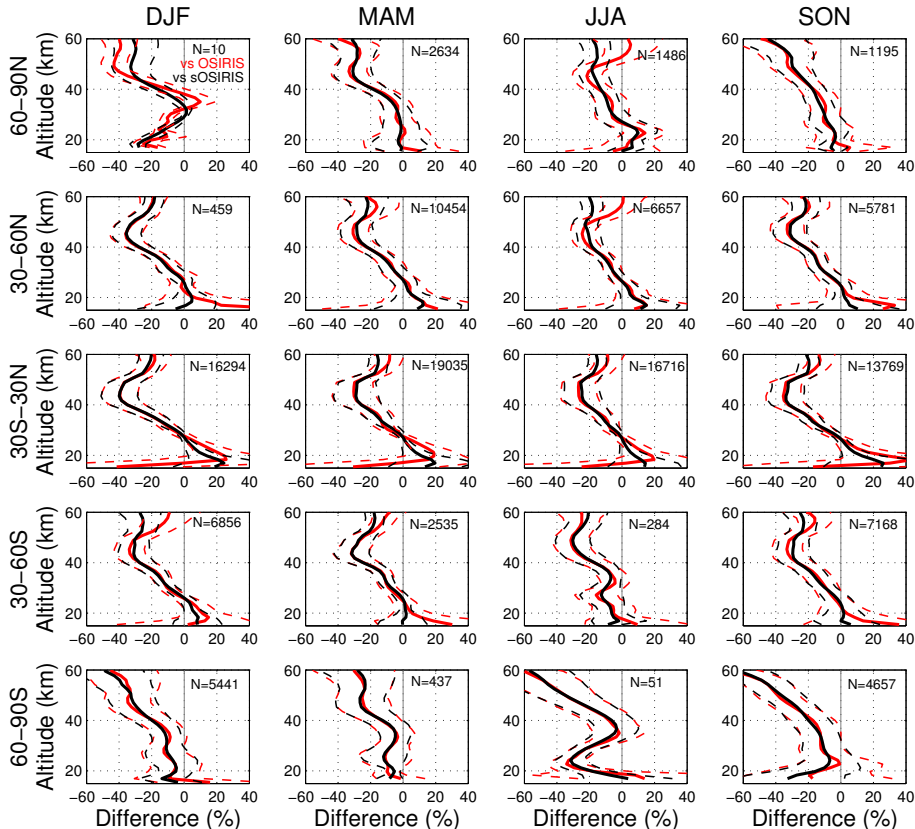


Figure 3. As Fig. 2, but for the mean relative differences (%) between GOME-2 and OSIRIS ozone profiles.

**GOME-2/Metop-A
ozone profile
comparison**

A. Määttä et al.

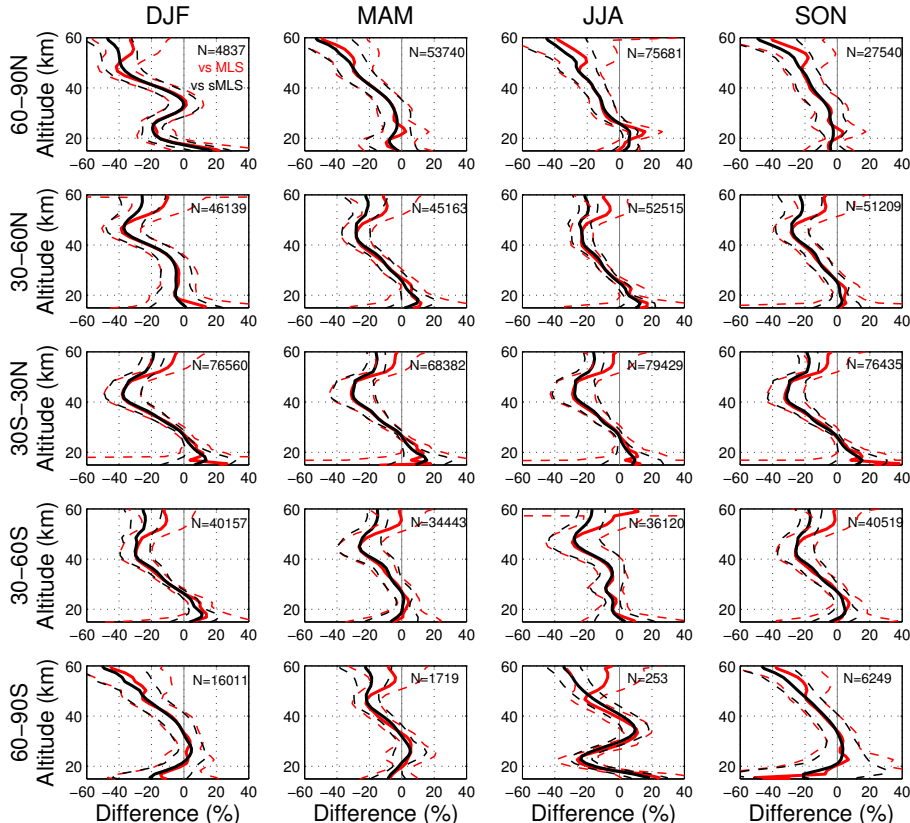


Figure 4. As Fig. 2, but for the mean relative differences (%) between GOME-2 and MLS ozone profiles.

[Title Page](#)[Abstract](#)[Introduction](#)[Conclusions](#)[References](#)[Tables](#)[Figures](#)[◀](#)[▶](#)[◀](#)[▶](#)[Back](#)[Close](#)[Full Screen / Esc](#)

**GOME-2/Metop-A
ozone profile
comparison**

A. Määttä et al.

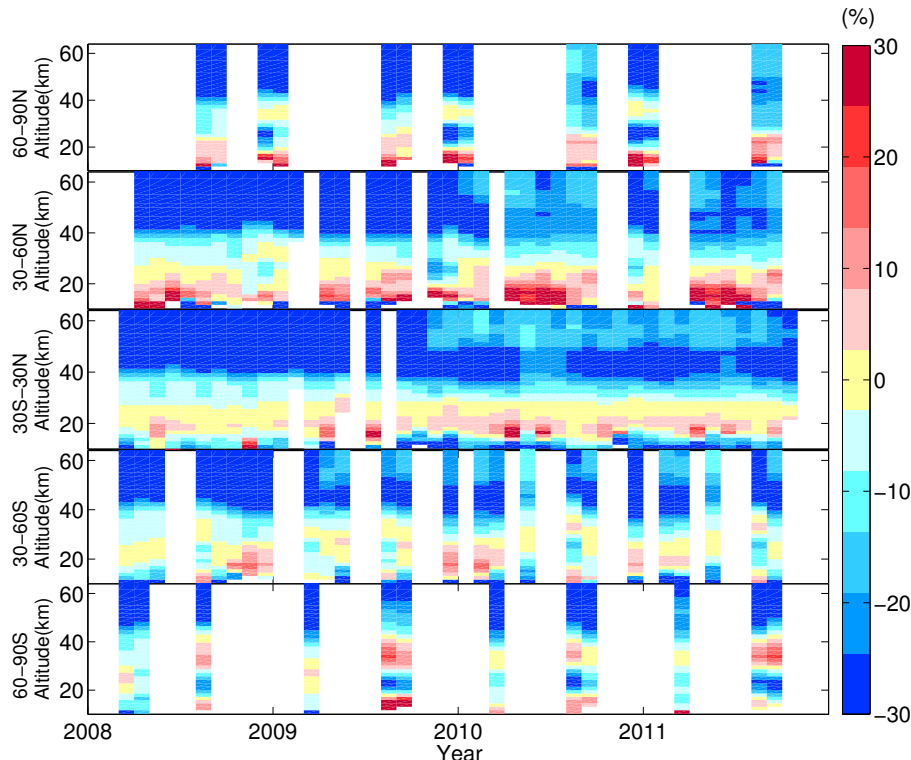


Figure 5. Monthly median relative differences between GOME-2 and smoothed GOMOS ozone profiles, in different latitude zones in the time period of 2008–2011. The monthly median is missing if there are less than ten collocated profiles.

**GOME-2/Metop-A
ozone profile
comparison**

A. Määttä et al.

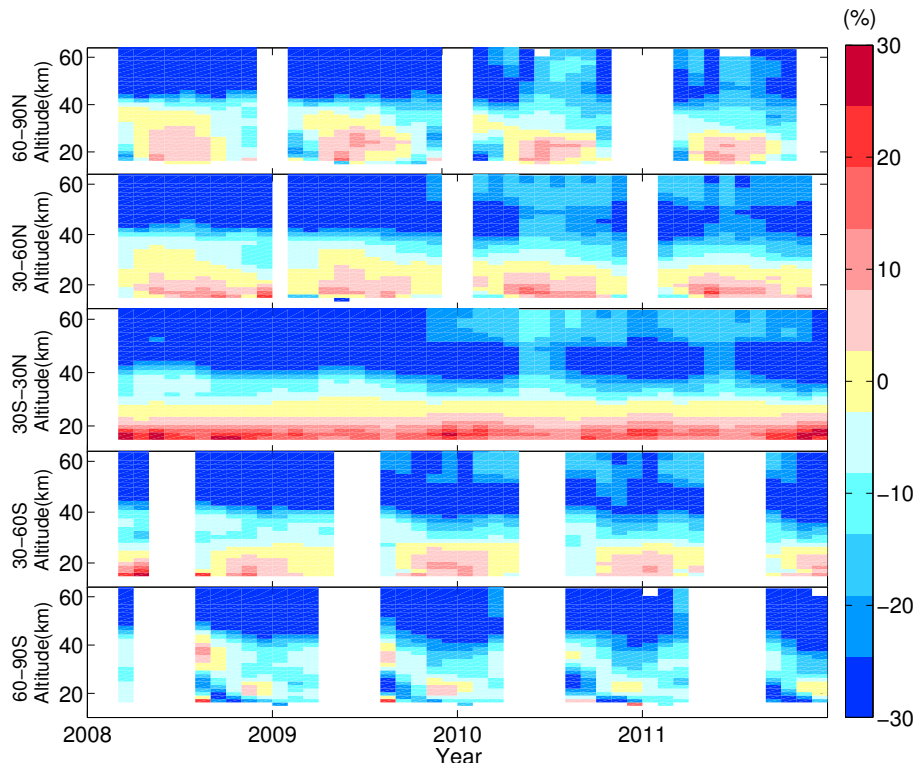


Figure 6. As Fig. 5, but for the monthly median relative differences between collocated GOME-2 and smoothed OSIRIS ozone profiles.

- [Title Page](#)
- [Abstract](#) | [Introduction](#)
- [Conclusions](#) | [References](#)
- [Tables](#) | [Figures](#)
- [◀](#) | [▶](#)
- [◀](#) | [▶](#)
- [Back](#) | [Close](#)
- [Full Screen / Esc](#)
- [Printer-friendly Version](#)
- [Interactive Discussion](#)

**GOME-2/Metop-A
ozone profile
comparison**

A. Määttä et al.

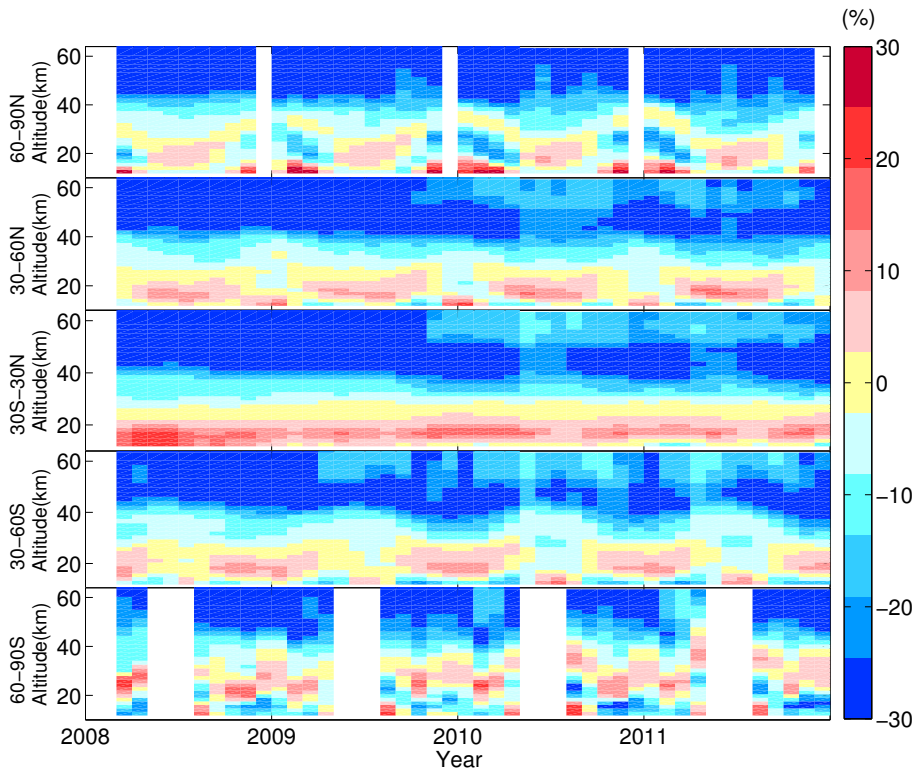


Figure 7. As Figs. 5 and 6, but for the monthly median relative differences between collocated GOME-2 and smoothed MLS ozone profiles.

**GOME-2/Metop-A
ozone profile
comparison**

A. Määttä et al.

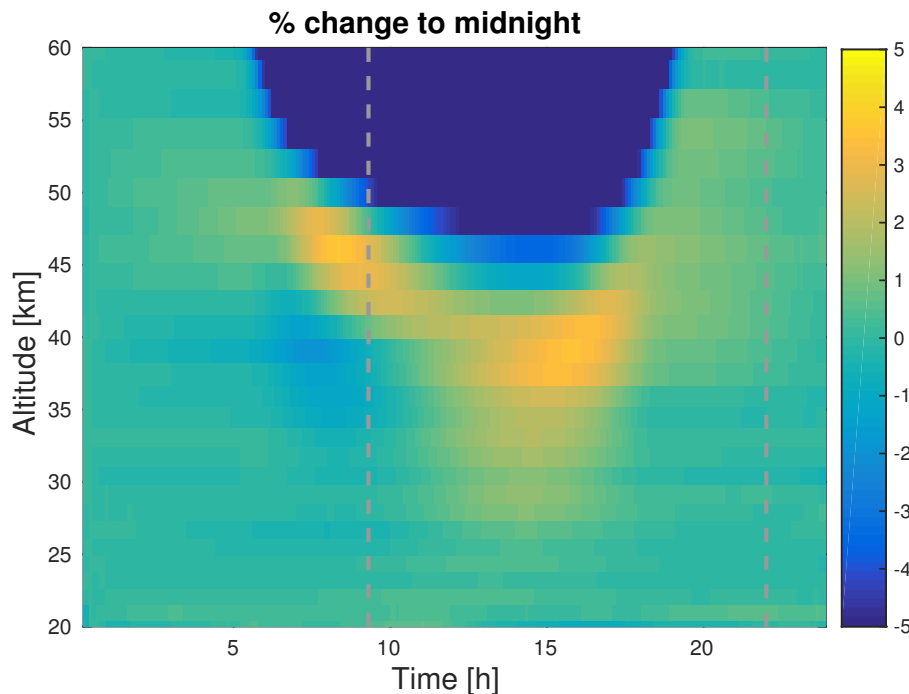


Figure 8. The diurnal variation of ozone illustrated by the Whole Atmosphere Community Climate Model (WACCM). The local solar times of GOME-2 and GOMOS measurements are marked with dashed vertical lines.

**GOME-2/Metop-A
ozone profile
comparison**

A. Määttä et al.

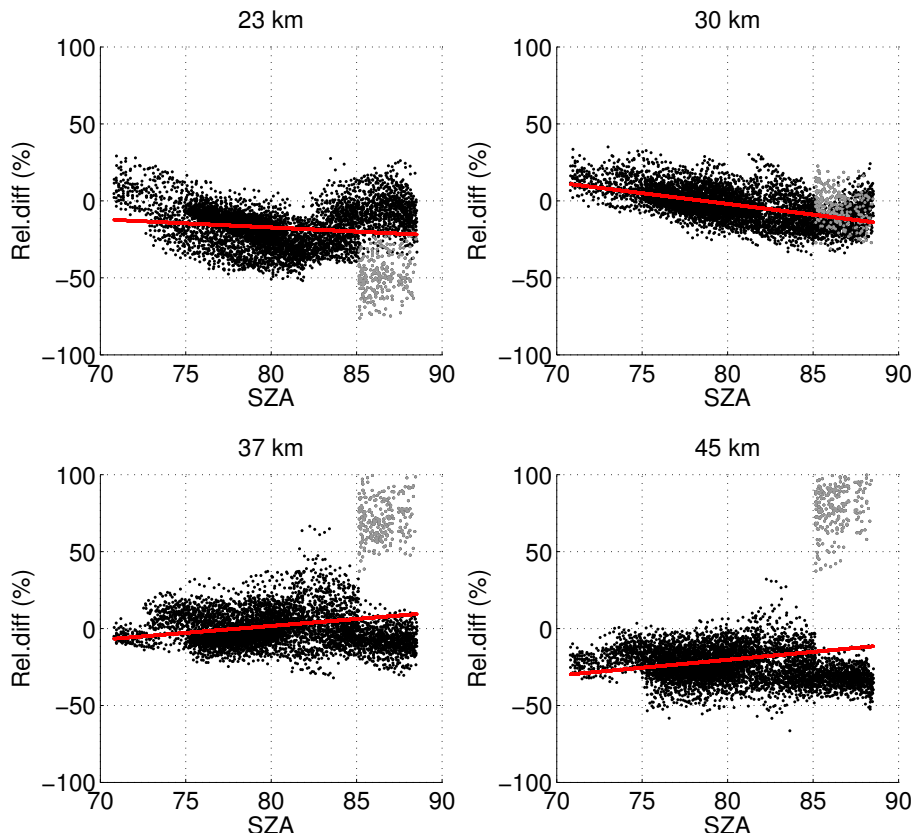


Figure 9. The relative differences (%) with respect to smoothed GOMOS profiles as a function of SZA, at four altitude layers around 23 km (upper left), 30 km (upper right), 37 km (bottom left) and 45 km (bottom right). The profiles are from the southern high latitudes ($60\text{--}90^\circ\text{ S}$) covering one year 2010 of comparison data. The grey dots represent pixels having high disagreement with ozone vertical distribution.

**GOME-2/Metop-A
ozone profile
comparison**

A. Määttä et al.

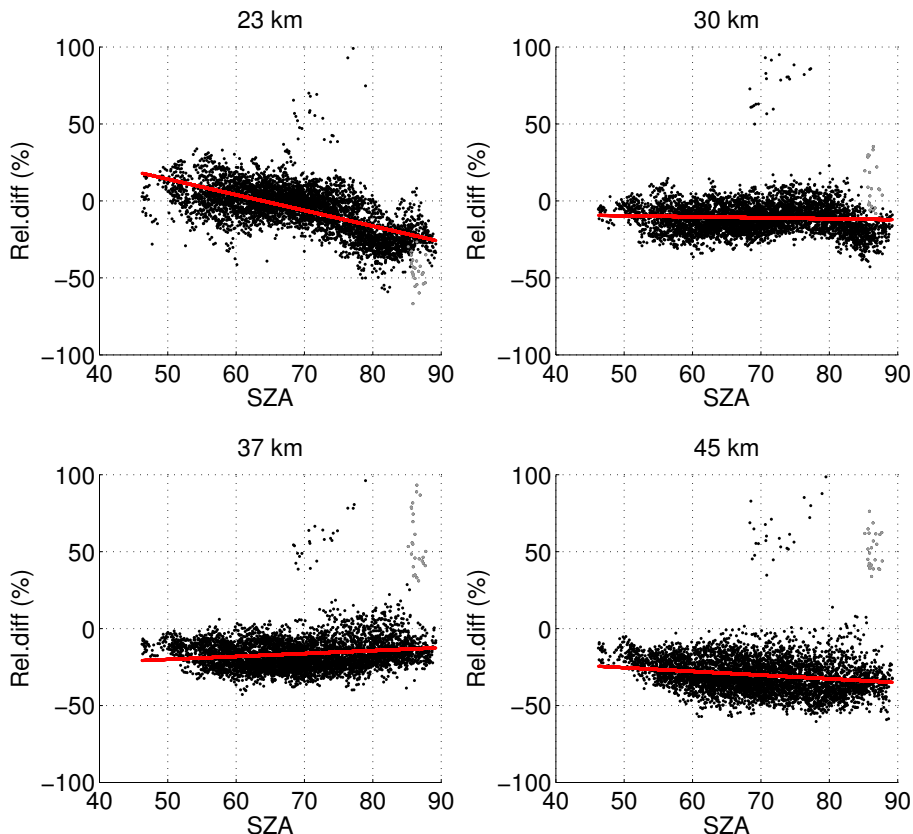


Figure 10. As Fig. 9, but against smoothed OSIRIS profiles, at four altitude layers.

GOME-2/Metop-A ozone profile comparison

A. Määttä et al.

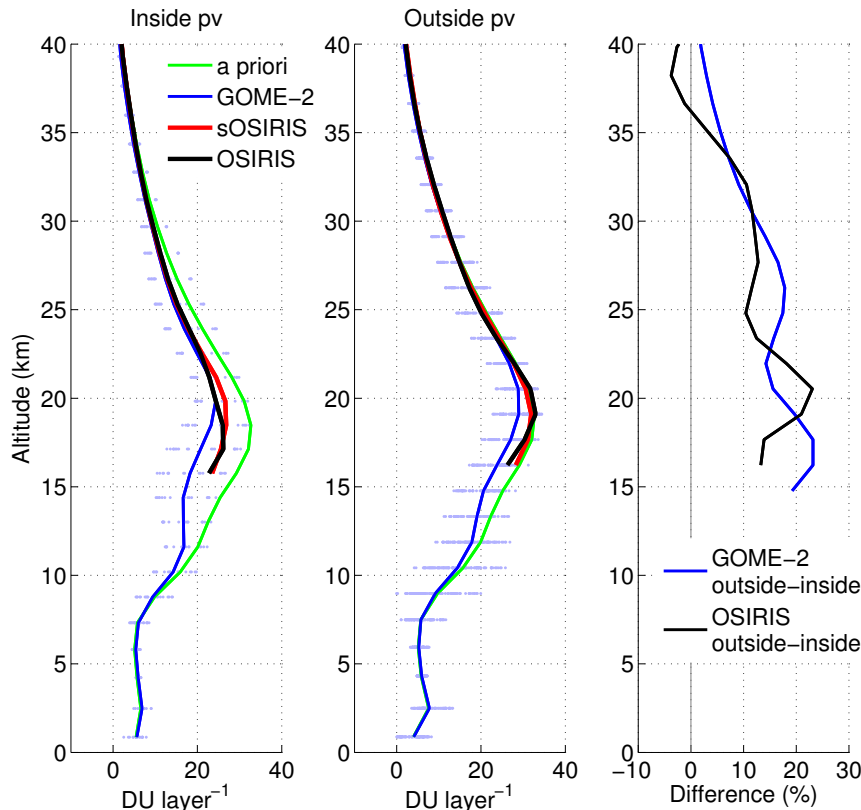


Figure 11. Monthly averages of the collocated GOME-2 (blue), OSIRIS (black), smoothed OSIRIS (red) and a priori (green) ozone profiles inside polar vortex (left panel) and outside polar vortex (middle panel) in the high northern latitudes ($60\text{--}90^\circ\text{N}$) in March 2011. The individual GOME-2 ozone amounts at each altitude layer are denoted by blue dots. The relative differences (%) between outside and inside polar vortex monthly means for GOME-2 and OSIRIS are shown in the right panel.

**GOME-2/Metop-A
ozone profile
comparison**

A. Määttä et al.

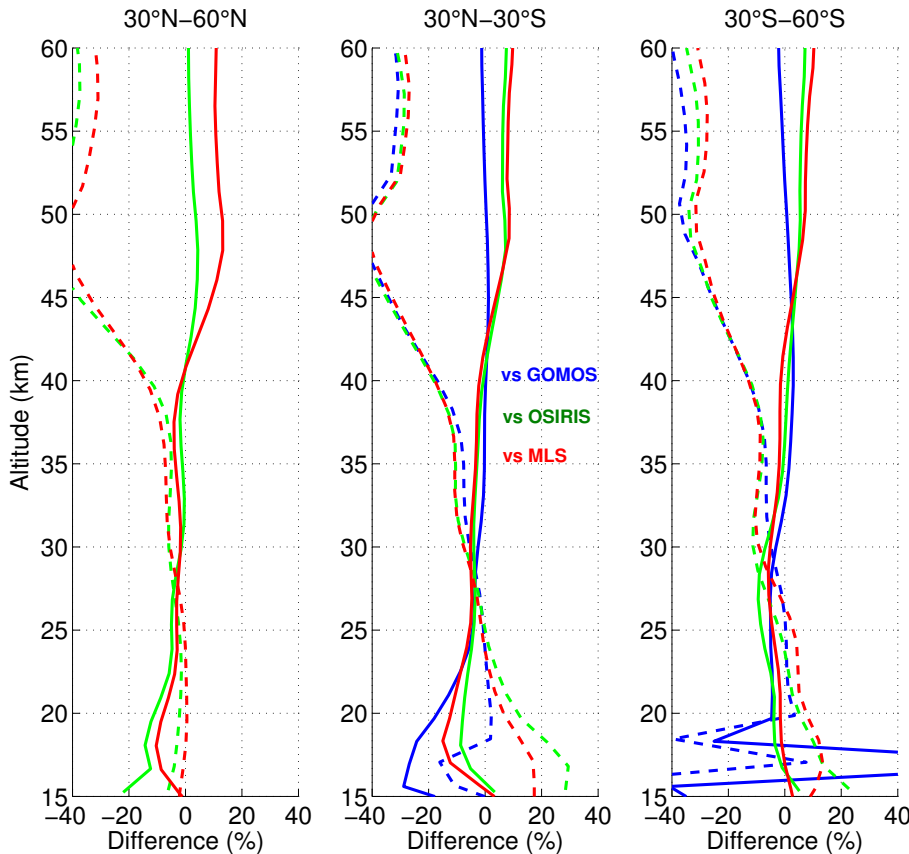


Figure 12. Monthly averages of the relative differences (%) with respect to the collocated smoothed GOMOS (blue), OSIRIS (green) and MLS (red) ozone profiles in March 2008. The results are shown for three latitude zones separately when using original operational GOME-2 data (dashed curves) and data using the new experimental correction for instrumental degradation (solid curves).